Suppression of fast relaxation and the Raman coupling coefficient in densified silica

2004 J. Phys.: Condens. Matter 16 3035

(http://iopscience.iop.org/0953-8984/16/18/004)

INSTITUTE OF PHYSICS PUBLISHING JOURNAL OF PHYSICS: CONDENSED MATTER

J. Phys.: Condens. Matter **16** (2004) 3035–3040 PII: S0953-8984(04)75149-8

Suppression of fast relaxation and the Raman coupling coefficient in densified silica

N V Surovtsev[1], V K Malinovsky[1], Yu N Pal'yanov[2], A A Kalinin[2] and A P Shebanin[2]

[1] Institute of Automation and Electrometry, Russian Academy of Sciences, Novosibirsk, 630090, Russia
[2] United Institute of Geology, Geophysics, and Mineralogy, Russian Academy of Sciences, Novosibirsk, 630090, Russia

Received 18 January 2004, in final form 16 March 2004
Published 23 April 2004
Online at stacks.iop.org/JPhysCM/16/3035
DOI: 10.1088/0953-8984/16/18/004

Abstract

Low-frequency Raman spectra of normal and pressure-densified silica are investigated. Strong suppression of fast relaxation intensity is found in densified silica in comparison with the normal type, the dependence of the fast relaxation intensity versus the density changing its behaviour near the density of the low-density crystalline SiO_2 polymorphs. The light–vibration coupling coefficients extracted from the comparison of Raman spectra and the vibrational density of states are different for densified and normal silica. In the case of the most densified sample, the position of the boson peak maximum marks the transition from the square frequency behaviour of the coupling coefficient to the linear one.

Spectral characteristics of terahertz dynamics of glasses consist of two main contributions—the so-called boson peak and fast relaxation. Investigation of these dynamics is the one of most interesting problems in the physics of condensed matter. The origin and detailed description of the boson peak and fast relaxation are matters of debate. One of the promising topics in modern studies is the investigation of densified silica, since this substance has a high frequency for the boson peak position, which facilitates spectroscopic investigations [1]. Raman [2], neutron [3], inelastic x-ray scattering [1, 4, 5], specific heat data [6], and also results of molecular dynamics simulation [7] are available now for the boson peak in densified silica. However, some interesting and important experimental information concerning the terahertz dynamics of densified silica is still lacking—to our knowledge, for densified silica there are no studies of the fast relaxation and of the behaviour of the Raman coupling coefficient, which relates the density of vibrational states to the Raman intensity [8]. The importance of studying the Raman coupling coefficient is argued in [9], with a short introduction.

In the present paper, the results of the investigation of low-frequency Raman spectra for densified silica with an emphasis on the behaviour of fast relaxation and the extraction of the Raman coupling coefficient are reported. The abrupt decrease in apparent intensity of fast

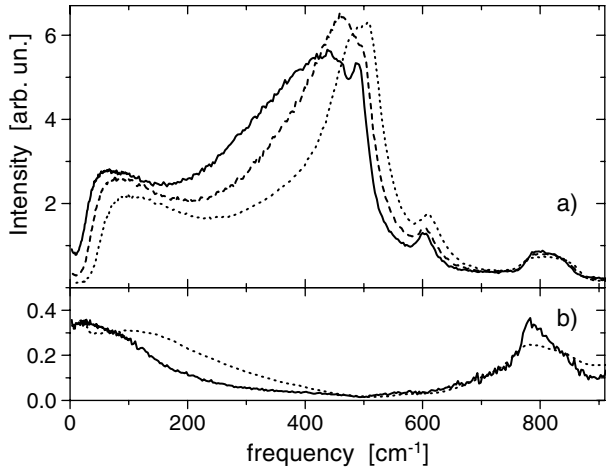

Figure 1. (a) Polarized Raman spectra of normal and densified silica: N-sample (solid curve), M-sample (dashed curve), and D-sample (dotted curve). (b) The depolarized ratio.

relaxation is found for densified silica. Also, the coupling coefficient for densified silica reveals a frequency behaviour different from that of usual glasses—a square frequency dependence is found for the spectral range just below the boson peak maximum.

A set of five densified samples was produced by application of high-temperature, high-pressure conditions to silica cylinders of height and diameter 4 mm using a high-pressure apparatus of 'split sphere' type (BARS) [10] and rapid temperature quenching to the ambient value. Details of the calibration of P–T parameters have been presented elsewhere [11]. The density of the densified samples was determined by weighing in a liquid with the precision of 0.02 g cm^{-3}. The degree of densification depends on applied temperature, pressure, and, to a minor extent, compression time. So, starting from the normal density of 2.22 g cm^{-3}, the sample retrieved after 20 h at $P = 50$ kbar, $T = 550\,^{\circ}$C has the density of 2.45 g cm^{-3}, while the sample quenched after 20 h at $P = 70$ kbar, $T = 650\,^{\circ}$C has the density of 2.68 g cm^{-3}. For the rest of the paper, these samples will be called the N-sample, M-sample, and D-sample, respectively. Other samples had intermediate characteristics in comparison with these samples.

Polarized (VV) and depolarized (HV) Raman right-angle experiments were performed using an argon ion laser with a wavelength of 514.5 nm, a power of 400 mW, and a double-grating monochromator U-1000. For the low-frequency part ($<$100 cm^{-1}) of the spectra, spectral slits of 1.5 cm^{-1} were used. The experiments were conducted at room temperature and at 95 K applying a liquid nitrogen cryostat. In the latter case, the temperature on the illuminated part of the samples was determined from the Stokes to anti-Stokes ratio.

Polarized Raman spectra of three representative samples are shown in figure 1(a), where the normalization of the spectral intensity by the integral over a mode near 800 cm^{-1} is used. This normalization implies the assumption that the number of silicon–oxygen stretching vibrations, with which this band is associated [12], and their strength of coupling to the polarized spectrum do not undergo significant changes upon densification. It is seen from figure 1 that the low-frequency part of the boson peak is suppressed for denser silica glasses, while the high-frequency part approaches the common asymptote. This picture of the boson peak in densified silica is similar to that found for the vibrational density of states by neutron scattering [3]—the main effect of densification is the suppression of the density of states at low energy. Also, a sharp decrease in the Raman scattering intensity in the range $<$10 cm^{-1}, where the fast relaxation spectrum dominates, is noticeable in figure 1(a). The Raman signal at $\nu = 10$ cm^{-1} for the D-sample is 7.3 times lower than for the normal silica.

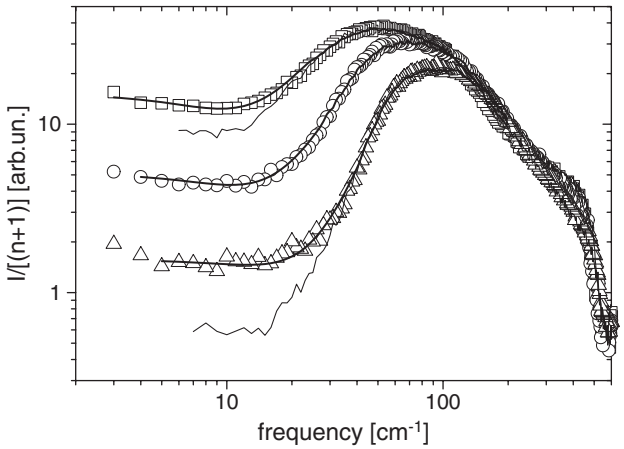

Figure 2. A reduced presentation of the low-frequency depolarized Raman spectra: N-sample (squares), M-sample (circles), and D-sample (triangles). The thin curves show the spectra at $T = 95$ K and the thick curves refer to the fit with equation (1).

Note, in the case of the depolarized spectra, that the normalization by the 800 cm^{-1} band does not lead to a picture consistent with neutron results. The reason is the difference in depolarization ratio between normal and densified silica, as is shown in figure 1(b), also in the range of the 800 cm^{-1} band. That is why the depolarized low-frequency Raman spectra are shown in figure 2 with normalization by the high-frequency part of the boson peak. Here the spectra are displayed in the reduced presentation $I_n(\nu) = I(\nu)/[(n+1)\nu]$, removing the trivial temperature dependence for the vibrational spectrum (n is the Bose factor). Low-temperature spectra added to this figure allow us to separate the changes in the vibrational spectrum from the relaxational contribution, which increases with temperature faster than the Bose factor. It is seen from figure 2 that silica densification leads not only to the suppression of the low-energy part of the boson peak but also to the suppression of the fast relaxation intensity.

For the quantitative description of fast relaxation, we used the model of a damped oscillator [13–16]. Within this model, fast relaxation is manifested in the light scattering spectra as a relaxational part of the response of boson peak vibrations. Since the single relaxational time is a good approximation for the silica glass at room temperature [17], the low-frequency Raman spectrum is written in the model of a damped oscillator as [16]

$$I_n(T,\nu) = \frac{2}{\pi}\int_0^\infty \frac{I_n^\nu(T,\Omega)\Omega^2\delta^2\gamma/\left(\nu^2+\gamma^2\right)\,\mathrm{d}\Omega}{\left(\Omega^2-\nu^2-\delta^2\gamma^2/\left(\nu^2+\gamma^2\right)\right)^2+\left(\delta^2\gamma\nu/\left(\nu^2+\gamma^2\right)\right)^2}, \quad (1)$$

where I_n^ν is the vibrational spectrum, δ^2 is the damping parameter, and γ is the width of the relaxational spectrum related to the relaxational time τ via $\gamma = 1/(2\pi\tau)$. In the hydrodynamic approximation, the damping parameter has a square dependence on frequency:

$$\delta^2 = \delta_0^2\Omega^2, \quad (2)$$

where δ_0^2 is just proportional to the integral over the relaxational part of the spectrum [16].

The experimental spectra were fitted by equations (1), (2). As for the vibrational spectrum, there the low-temperature spectra were used with extrapolation using a power law at very low frequencies where the contribution of fast relaxation is seen even at $T = 95$ K. The results for the parameters δ_0^2 and τ are plotted in figure 3 versus the density. The result of fitting for the spectrum of a silica sample irradiated by fast neutrons (the so-called metamict phase; a spectrum from [18]) is also added to this figure. It is seen that, while τ has a gradual decrease as the density increases, the integral over the fast relaxational spectrum has a gradual decrease only for densities above $\sim$2.26 g cm^{-3}, the value being close to that for the low-density crystalline SiO_2 polymorphs (the densities of tridymite and cristobalite are 2.26 and

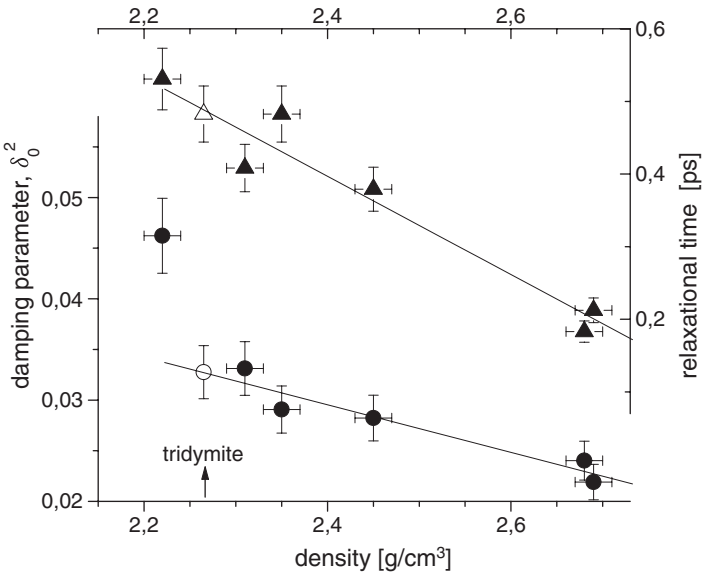

Figure 3. Parameters of the fast relaxational spectrum versus the sample density: δ_0^2 (circles, left axis) and relaxational time (triangles, right axis). The open symbols correspond to the metamict sample from [18]. The lines are linear fits for metamict and densified samples.

2.30 g cm^{-3}, respectively). This finding has a natural explanation under the assumption of an inhomogeneous glassy structure. In this case, the local packing of SiO_4 tetrahedra has favourable structures such as cristobalite and tridymite and more disordered, less dense places, which play the role of relaxation centres. There are many works where the interrelation between silica and low-density crystalline SiO_2 polymorphs is suggested; see, for example, [19, 20]. The first stage of densification is mainly related to the decrease in the number of weak, highly disordered places and, therefore, leads to a significant decrease in integral strength of the fast relaxation spectrum. Densification to densities higher than that of the low-density crystalline SiO_2 polymorphs is related to the change in the type of local favourable ordering to the direction of quartz, leading to a much slower decrease in fast relaxation as the density increases. Thus, our finding supports the viewpoint that there is a tendency of local structure of silica to take an ordering similar to that of the low-density crystalline SiO_2 polymorphs.

The assumption that the same relaxation is responsible for the appearance of fast relaxation in the Raman spectra and for broadening of the Brillouin line [15, 17] allows one to calculate the prediction for the Brillouin linewidth using directly the parameters found in the low-frequency Raman spectrum fit. Note that this estimation has smaller error bars than these shown in figure 3, since the product $\delta_0^2\gamma$ is determined in the fit with much higher precision than these parameters separately (this combination is responsible for the zero-frequency limit in the spectral density presentation). The parameters presented in figure 3 predict the width of 181 MHz at 33.7 GHz for normal silica and 49 MHz at 41.5 GHz for the D-sample. These values are in reasonable agreement with those found experimentally at these frequencies: 142 ± 7 MHz for normal silica [21] and 52 ± 10 MHz for densified silica with $\rho \approx 2.6$ g cm^{-3} [22]. This agreement supports the assumption of the same origin of the fast relaxational processes revealed in Raman and Brillouin scattering.

To calculate the light–vibration coupling coefficient in the Shuker–Gammon formula [8] for N- and D-samples, we used our low-temperature Raman data and the density of the

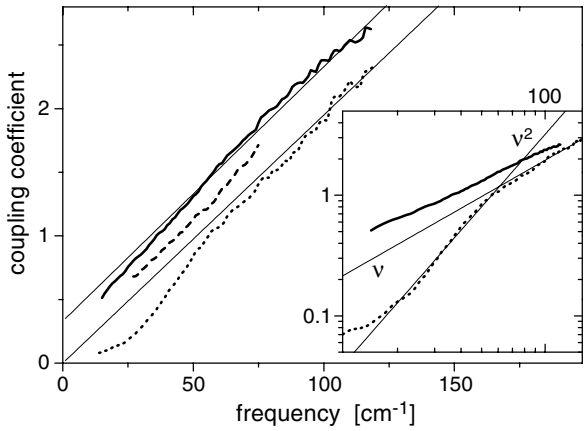

Figure 4. The frequency dependence of the Raman coupling coefficient of normal and densified silica (same legend as in figure 1). The upper thin line is the behaviour found for silica glass in [25] and the lower one is $\propto\nu$. The inset shows the coupling coefficient of the N- and D-samples in logarithmic presentation. Thin lines here are linear and square frequency behaviours.

vibrational state found from figure 3 of [3] for similar silica samples. For the M-sample, the density of vibrational states was calculated by Tikhonov's regulation method (in the way described in [23]) from low-temperature data of [6] where a densified silica sample of the same density was studied. The results for the Raman coupling coefficient for three silica samples are shown in figure 4. It is seen that densification leads to a decrease in the Raman coupling coefficient. Whereas the N-sample follows well the linear frequency behaviour near the boson peak maximum with a nonvanishing value for zero-frequency extrapolation, which was found for silica glass [24, 25] and also for a number of other glasses [26, 25] (small deviations from results of [24, 25] are attributed to the precision of the data for the vibrational density of states in [3]), the coupling coefficient of the M-sample appears to show a decrease in the frequency constant contribution. This is in contrast with the results of [27], where rescaling of the coupling coefficient relative to the boson peak maximum leads to identical behaviour for samples with different thermal histories.

Further densification of silica results in the change in the linear frequency behaviour to a square frequency one just below the boson peak maximum ($\nu_{\mathrm{BP}} \sim 64$ cm^{-1} for the most densified sample in [3]). We used the definition of the boson peak maximum ν_{BP} as the maximum position for the density of vibrational states divided by square frequency. The square frequency dependence of the coupling coefficient is associated with light scattering from attenuated acoustic plane waves [28], while the linear behaviour usually found for glasses near the boson peak maximum [25] needs another interpretation. The diffuse-like behaviour of strongly scattered vibrational excitations could produce the linear behaviour of the coupling coefficient [27, 29]. Therefore, the results presented in figure 4 support the conclusion drawn in [4, 22] that the position of the boson peak maximum in densified silica coincides with the frequency of crossover to the strong scattering of acoustic excitations.

For usual glasses, the transition to the superlinear behaviour is observed at a frequency of 0.3–0.5ν_{BP} [25]. However, for the D-sample this transition coincides with ν_{BP}. We believe that the above mentioned quantitative difference between densified silica and normal glasses emphasizes that results found for highly densified glasses should be extended to other glasses with caution. For example, while the position of the crossover frequency Ω_{co} is found to coincide with the boson peak maximum for densified silica [4, 22], this coincidence would not hold for normal silica. Ω_{co} is expected to be reflected in the coupling coefficient as a transition from superlinear to linear frequency behaviour. If this is true, the estimate of the crossover frequency is $\Omega_{\mathrm{co}} \approx 0.3\nu_{\mathrm{BP}}$ for normal silica. A relatively high frequency of the crossover in the case of the D-sample allows us to observe superlinear behaviour for almost

one order of magnitude in intensity and to establish the square frequency behaviour of the coupling coefficient with high precision.

To conclude, the low-frequency Raman spectra of densified silica glasses reveal a striking suppression of the fast relaxation intensity as the sample density increases. Described by the damped oscillator model, the Raman spectra give evidence that the integral fast relaxation intensity decreases rapidly in the range up to the density of the low-density crystalline SiO_2 polymorphs and slowly at higher densities, supporting the assumption that the local ordering of the silica structure has similarity with that of the low-density polymorphs. The light–vibration coupling coefficient demonstrates the suppression of the low-frequency part for densified silica and the change of the linear frequency behaviour to the square frequency just below the boson peak maximum. The relative facility of access to this spectral range together with the low level of fast relaxation in densified silica makes densified silica a very attractive object for studies of vibrational excitations just below the crossover to strong scattering.

Acknowledgment

This work was supported by the Interdisciplinary Science Fund at the Russian Foundation for Basic Research of the Siberian Branch of the Russian Academy of Sciences (project No 140).

References

[1] Rat E, Foret M, Courtens E, Vacher R and Arai M 1999 *Phys. Rev. Lett.* **83** 1355
[2] Sugai S and Onodera A 1996 *Phys. Rev. Lett.* **77** 4210
[3] Inamura Y, Arai M, Nakamura M, Otomo T, Kitamura N, Bennington S M, Hannon A C and Buchenau U 2001 *J. Non-Cryst. Solids* **293–295** 389
[4] Foret M, Vacher R, Courtens E and Monaco G 2002 *Phys. Rev.* B **66** 024204
[5] Rufflé B, Foret M, Courtens E, Vacher R and Monaco G 2003 *Phys. Rev. Lett.* **90** 095502
[6] Liu X, von Löhneysen H, Weiss G and Arndt J 1995 *Z. Phys.* B **99** 49
[7] Pilla O, Angelani L, Fontana A, Gonçalves J R and Ruocco G 2003 *J. Phys.: Condens. Matter* **15** S995
[8] Shuker R and Gammon R W 1970 *Phys. Rev. Lett.* **25** 222
[9] Surovtsev N V, Adichtchev S V, Rössler E and Ramos M A 2004 *J. Phys.: Condens. Matter* **16** 223
[10] Pal'yanov Yu N, Khokhryakov A F, Borzdov Yu M, Sokol A G, Gusev V A, Rylov G M and Sobolev N V 1997 *Russ. Geol. Geophys.* **38** 920
[11] Pal'yanov Yu N, Sokol A G, Borzdov Yu M and Khokhryakov A F 2002 *Lithos* **60** 145
[12] McMillan P, Piriou B and Couty R 1984 *J. Chem. Phys.* **81** 4234
[13] Winterling G 1975 *Phys. Rev.* B **12** 2432
[14] Gochiyaev V Z, Malinovsky V K, Novikov V N and Sokolov A P 1991 *Phil. Mag.* B **63** 777
[15] Sokolov A P, Novikov V N and Strube B 1997 *Europhys. Lett.* **38** 49
[16] Novikov V N, Sokolov A P, Strube B, Surovtsev N V, Duval E and Mermet A 1997 *J. Chem. Phys.* **107** 1057
[17] Wiedersich J, Adichtchev S V and Rössler E 2000 *Phys. Rev. Lett.* **84** 2718
[18] Malinovsky V K, Novikov V N, Surovtsev N V and Shebanin A P 2000 *Phys. Solid State* **42** 65
[19] Dove M T, Harris M J, Hannon A C, Parker J M, Swainson I P and Gambhir M 1997 *Phys. Rev. Lett.* **78** 1070
[20] Nakamura M, Arai M, Otomo T, Inamura Y and Bennengton S M 2001 *J. Non-Cryst. Solids* **293–295** 377
[21] Pelous J and Vacher R 1975 *Solid State Commun.* **16** 279
[22] Courtens E, Foret M, Hehlen B, Rufflé B and Vacher R 2003 *J. Phys.: Condens. Matter* **15** S1279
[23] Surovtsev N V 2001 *Phys. Rev.* E **64** 061102
[24] Fontana A, Dell'Anna R, Montagna M, Rossi F, Viliani G, Ruocco G, Sampoli M, Buchenau U and Wischnewski A 1999 *Europhys. Lett.* **47** 56
[25] Surovtsev N V and Sokolov A P 2002 *Phys. Rev.* B **66** 054205
[26] Fontana A, Righetti L, Rossi F, D'Angelo G, Börjesson L, Matic A, Cicognani G and Dianoux A J 2002 *Phil. Mag.* B **82** 257
[27] Surovtsev N V, Shebanin A P and Ramos M A 2003 *Phys. Rev.* B **67** 024203
[28] Jäckle J 1981 *Amorphous Solids: Low-Temperature Properties* ed W A Phillips (Berlin: Springer) p 135
[29] Novikov V N 1994 *Proc. 14th Int. Conf. on Raman Scattering* ed N-T Yu and X-Y Li (New York: Wiley) p 766